Synthesis and Characterization of Activated Carbons from Avocado Kernel; Application to Phenol Removal

Taba To'Ora Kaga, Kwamivi Nyonuwosro Segbeaya, Virginie Pallier, Geneviève Feuillade

American Journal of Materials Science and Engineering, 2024, Vol. 12, No. 1, 1-12
Available online at http://pubs.sciepub.com/ajmse/12/1/1
Published by Science and Education Publishing
DOI:10.12691/ajmse-12-1-1

Synthesis and Characterization of Activated Carbons from Avocado Kernel; Application to Phenol Removal

Taba To'ora Kaga[1,2,3,*], Kwamivi Nyonuwosro Segbeaya[1,2], Virginie Pallier[3], Geneviève Feuillade[3]

[1]Laboratory of Waste Treatment and Recovery Management, Faculty of Sciences, University of Lomé, Togo
[2]Organic Chemistry and Environmental Science Laboratory, University of Kara, Togo
[3]Water and Environment Limoges, ENSIL-ENSCI, University of Limoges, France
*Corresponding author: pascalkaga@gmail.com

Received December 01, 2023; Revised Januaryr 02, 2024; Accepted January 09, 2024

Abstract Water pollution is characterized by the presence of a wide variety of substances found in significant quantities in this environmental compartment, which requires the installation of high-performance treatments. Among the multiple technics of treatment, one can mention the adsorption on activated carbons which enable the retention of organic molecules. This led to the development of high-cost granular activated carbons to specifically reduce some micro-pollutants or macro-molecules. This work aims at designing a low-cost activated carbon adsorbent material by giving it properties to adsorb a broad spectrum of the pollutant load of effluents rich in organic molecules such as landfill leachate. The first phase of this study involved the synthesis of activated carbon from avocado core with optimization of manufacturing conditions, followed by physical and chemical characterization. Activated carbon with the highest iodine index value (1506 $mg.g^{-1}$) and the highest specific surface area (862 $m^2.g^{-1}$) was obtained. FTIR results confirms the presence of carboxylic functional groups, lactones and phenols. Phenol removal tests were carried out in batch mode to evaluate the adsorbent performance. Results showed that equilibrium was reached during a contact time of 60 min for an adsorption capacity of 48 $mg.g^{-1}$. The study of adsorption kinetics revealed the adequacy of the pseudo-second order kinetic model. These results show that avocado kernels would be good adsorbent for organic compounds in solution.

Keywords: *avocado kernels, adsorption, activated carbon, leachate*

Cite This Article: Taba To'ora Kaga, Kwamivi Nyonuwosro Segbeaya, Virginie Pallier, and Geneviève Feuillade, "Synthesis and Characterization of Activated Carbons from Avocado Kernel; Application to Phenol Removal." *American Journal of Materials Science and Engineering*, vol. 12, no. 1 (2024): 1-12. doi: 10.12691/ajmse-12-1-1.

1. Introduction

Pollutants are constantly being discharged into the environment, generating a lot of organic and mineral residues. Over the past few years, research which has focused on previously neglected wastes, have shown that they can have added value through the production of second-generation materials. This approach has aroused interest in the development of new recovery processes, particularly those used for the production of adsorbents, which have experienced real boom [1]. Activated carbon is a material known for its high adsorption capacity and is one of the most commonly used materials in many liquid or gas phase applications, for its interesting structural properties (porosity, specific surface area, etc.). It is currently widely used in the industrial, healthcare and para pharmaceutical sector [2], as well as for water treatment. The structural properties and efficiency of activated carbon are highly related on the raw materials in their manufacture. However, it should be noticed that this efficiency is relative to the use for which it is intended, and consequently determines the choice of basic or raw materials [3]. The manufacturing of activated carbon, the expected performances in related to various uses go necessarily through the identification and choice of raw materials. They are mainly derived from carbon-containing materials of plant origin, such as cocoa pod shells [4] coconut shells, date pits [5], tea waste [6] wheat and rice [7], eucalyptus [8], animal waste (animal bones, blood and hair) or minerals waste (coal, coke, peat). The manufacturing process can be carried out by both physical and chemical activation. In general, the activation reaction is a process that uses an oxidizing agent at high temperature to produce a highly porous product. The physical activation follows two phases. The first phase, known as carbonization, is generally carried out at relatively moderate temperatures (400 to 500°C). The aim is to remove organic compounds and form a carbon. The material then undergoes extensive activation by treatment with steam, carbon dioxide or a mixture of these gases at 800°C [9,10]. The second phase leads to the opening of pores and the production of a very large specific surface area (between 500 and 3000 $m^2.g^{-1}$), whereas the original carbonisate generally has only a low specific surface area

(from 50 to 250 $m^2.g^{-1}$) [11].

In chemical activation, raw carbonaceous materials such as sawdust, peat, molasses and vegetable waste are mixed with chemicals such as sulfuric acid, calcium chloride, zinc chloride, phosphoric acid, potassium hydroxide, etc. After carbonization (400 to 500°C), the carbon is separated from the inorganic activating substance by dissolving the latter in a suitable washing. Zinc chloride [12-14] and phosphoric acid [15-17] are the activating agents most commonly used.

A number of parameters can be used to characterize activated carbon and determine conditions of use. These include pore volume and pore size, specific surface area, grain size, hardness, density, iodine number, ash content [3]. The main characteristics of activated carbons from different materials are compared in Table 1.

Table 1. main characteristics of activated carbons depending on source material (Carbochem, 2004)

Properties	Coal AC	Wood AC	Coconut AC	Lignite AC
Micro pores (number)	rich	poor	rich	medium
Macro pores (number)	medium	rich	poor	rich
Hardness	rich	poor	rich	poor
Density ($g.cm^{-3}$)	0.48	0.35	0.48	0.4 g
Iodine index	1000	1000	1100	600
Ash content	10%	5%	5%	20%
Manufacturing method	physical	chemical	physical	physical
Regeneration	Good	impossible	Good	bad

Recently, studies have focused on the conversion of agricultural and forestry biomass into value-added products, in particular adsorbents for the mitigation of environmental pollutants. For example, research has revealed the effectiveness of avocado kernel based activated carbon in the adsorption of phenolic compounds [12], cadmium ion [18], ammonium [19], methylene blue [20].

As part of our research into the valorization of Togolese biomass, we have turned our attention to avocado kernels for the production of activated carbon by chemical activation with orthohosphoric acid, with a view to manufacturing a new material composite for the treatment of waters with a high organic and mineral load. The choice was made not to produce an expensive material whose manufacturing process requires high-temperature pyrolysis, but to limit activation to the use of a chemical agent and a temperature rise around 500°C.

2. Materials and Methods

2.1. Raw Material, Origin and Uses

The avocado is the fruit of the avocado tree (*Persea americana*) of which the seed, commonly called the stone, is used for a variety of purposes, not only to renew plantations, but for its health and cosmetic benefits. Despite these applications, these avocado kernel end up in the Togolese environment as urban waste. Hence the advantage of recycling them, giving them another added value. The kernels were collected from fruit sellers in the town of Atakpame in the Plateaux region where they are abundant. In fact, these sellers would constitute the main intermediaries in the acquisition and recovery of avocado kernels.

Parameters such as moisture content, volatile matter and ash content complying with the AFNOR XP CEN/TS 14774-3, XP CEN/TS 15148, and AFNOR XP CEN/TS 14775 standards, have been determined in order to have immediate knowledge of the raw material.

Part of the entire proceedings, not an independent document. Please do not revise any of the current designations.

2.2. Preparation of Activated Carbons

Avocado kernels were washed with distilled water and then oven-dried at 110°C for 24 hours. They were then crushed in a blender and sieved until the fraction smaller than 1 mm was obtained; the retained grains are impregnated in a mass of orthophosphoric acid at 85% in aqueous solution, at an impregnation ratio of 2, for a period of 24 hours and pyrolysis was carried out in a nitrogen atmosphere. Figure 1 shows the various stages in the activated carbon preparation process.

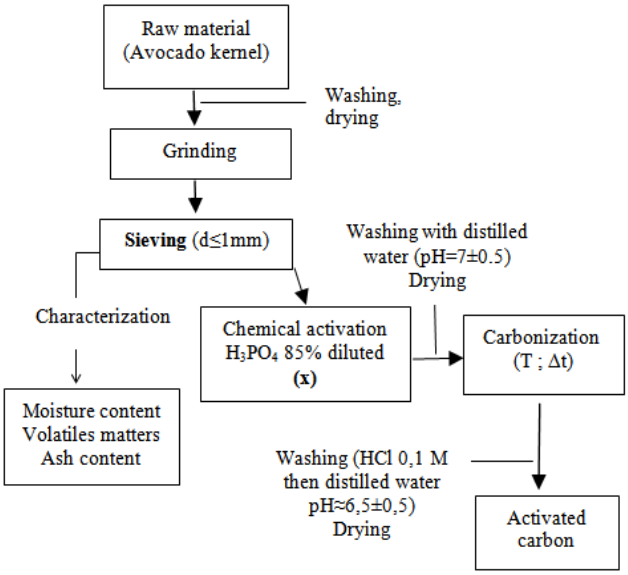

Figure 1. Schematic diagram of the activated carbon preparation process

In order to select the best activated carbon to meet the needs of this study, three parameters were studied during the synthesis process: carbonization temperature (T), carbonization time (Δt) and activating agent concentration (x). The eleven (11) activated carbons manufactured were coded according to the AC_T -Δt-x model where AC designates activated carbon, T represents the carbonization temperature, Δt is the carbonization duration and x is the activating agent concentration. The different carbons obtained according to the preparation conditions are shown in Table 2.

The choice of experimental conditions is justified by literature data, according to which several authors have shown that the advantage of chemical activation is low pyrolysis temperatures and lower energy cost. Good-quality activated carbons with a very large porous structure, high specific surface areas and a broad spectrum

of adsorbed molecules were prepared from plant biomasses using orthophosphoric acid as the chemical activating agent [21-23] which was also the choice made in this study.

Table 2. Activation and carbonization conditions

Coded	T (°C)	Δt (h)	x (%)
AC_{300}-2-50	300	2	50
AC_{350}-2-50	350	2	50
AC_{400}-1-50	400	1	50
AC_{400}-2-20	400	2	20
AC_{400}-2-35	400	2	35
AC_{400}-2-50	400	2	50
AC_{400}-2-65	400	2	65
AC_{400}-3-50	400	3	50
AC_{400}-4-50	400	4	50
AC_{450}-2-50	450	2	50
AC_{500}-2-50	500	2	50

2.3. Iodine Index of Activated Carbons

The iodine index was tested on all the prepared carbons in order to evaluate the influence of the preparation conditions of the activated carbons on this performance indicator and to identify optimal synthesis conditions. The purpose of the iodine index value test is to evaluate the porosity of an activated carbon; it's a precise and easy-to-implement test that approximates the specific surface area and provides information on the micro porosity of the carbons. This indicator was obtained using the AWWA B 600-78 standard method [16,24,25].

In addition, activated carbons preparation mass yields were calculated in order to assess the influence of mass loss on carbons performance.

2.4. Characterization of Activated Carbons

Table 3. Operating conditions for activated carbons characterization

Technical	Equipment	Operating conditions
IR spectroscopy	*Nicolet iS5 FTIR*, spectrum produced with 64 scans cumulative over the range from 4000 to 400 cm^{-1} with a resolution of 4 cm^{-1}	Formation of circular pellet 1 mm in diameter by compressed mixture under 7 atm of powders 150 mg KBr + 0.4 mg of sample
X-ray diffraction	*Brüker D8 ADVANCE ECO*, CuKα, λ= 1.5406 Å, 10 θ≤ 2θ ≤100θ, step 0.01θ; acquisition time 1h16mn	Deposition of powders on a sample holder and tamped surface with a glass slide so that it is flat and uniform
MEB	*MEB/EDS Hitachi TM3000*	Sample fixed to the surface of a black carbon pellet then placed on the sample holder
Specific surfaces S_{BET}	ASAP 2020 "micromeritics 2020"	Degassing 90°C for 1 hour then 350°C for 10 hours under vacuum

The authors use a number of parameters to characterize activated carbons. The pH at zero charge point (pH_{PCN}) determined by the Lopez-Ramon method [26], provides information on the pH of the aqueous solution in which the solid exists under zero electrical potential. Infrared spectrometry was used for qualitative determination of acidic or basic surface groups, while Boehm's method [27] was used for the quantitative determination. Chemical composition was determined by CHNS/O elemental analysis and activated carbons surfaces were observed by scanning electron microscopy (SEM). Finally, the crystalline phases are identified using X-ray diffraction. The specific surface area, which provides information on the total surface area per unit mass of adsorbent accessible to the molecules [28] was determined by the BET method. Equipment and operating conditions are summarized in Table 3 for some techniques.

2.5. Adsorption Capacity of Activated Carbon

In order to access the adsorption capacity of the activated carbon with the best performance indices, phenol adsorption was tested. In fact, due to its simple dosage, several authors [29-32] have been interested in this molecule to find out more about its adsorption capacities; the data in the literature therefore enable us to compare the effectiveness of the carbons synthesized in this study. Phenol (C_6H_6O, molar mass of 94 $g.mol^{-1}$) and its derivatives are among the European Union's priority pollutants and the United States Environmental Protection Agency [33].

Adsorption was followed until equilibrium time. The activated carbon/phenol solution mixture is stirred at defined time intervals in the range varying from 0 to 80 min. The tests were carried out in batch of 50 ml (20 mg of activated carbon for 2 mg of phenol in 50 ml of distilled water). The residual concentrations Ci, were determined on the filtrates by UV spectrophotometry at the wavelength λ_{max} = 270 nm and adsorbed quantity ($mg.g^{-1}$) is calculated using equation (1). Organic product concentration is given by Beer Lambert's law, from a calibration curve.

$$q_t = \frac{v(C_0 - C_i)}{m} \quad (1)$$

C_0 and C_i are respectively the initial and residual concentrations ($mg.l^{-1}$) of phenol; v the volume (l) of the solution; m the mass of the adsorbent (g).

To study the adsorption kinetics of phenol on carbon, pseudo-first order, pseudo-second order and intraparticle diffusion models were applied.

- Pseudo-first order kinetics

This kinetic model was proposed by Lagergren [34] and assumes that the adsorption at right time t is proportional to the difference between the quantity adsorbed at equilibrium and the quantity adsorbed at time t.

$$\frac{dq_t}{dt} = K_1.(q_e - q_t) \quad (2)$$

q_e and q_t are the quantities ($mg.g^{-1}$) of adsorbate adsorbed at equilibrium and at time t respectively and K_1 ($ml.min^{-1}$) is the adsorption rate constant.

After integration, equation (2) becomes:

$$ln(q_e - q_t) = lnq_e - K_1.t \quad (3)$$

- Pseudo-second order kinetics

This model assumes rapid adsorption of the solute at high-energy sites and relatively slow adsorption at low-energy sites.

The pseudo-second order kinetic model is expressed according to equation (4).

$$\frac{dq_t}{dt} = K_2.(q_e - q_t)^2 \quad (4)$$

q_e and q_t are the quantities (mg.g^{-1}) of adsorbate adsorbed at equilibrium and at time t respectively and K_2 (g.mg^{-1}.min^{-1}) is the adsorption rate constant.

Integrating equation (4), we obtain equation (5):

$$\frac{t}{q_t} = \frac{1}{K_2.q_e^2} + \frac{1}{q_e}t \quad (5)$$

• Intra-particle diffusion

The intra-particle diffusion model or Weber and Morris model assumes that the diffusion process is the only limiting step controlling adsorption.

$$q_t = K_d.t^{0,5} + C \quad (6)$$

K_3 is the intra-particle diffusion rate constant (mg.g^{-1}.min$^{-0.5}$) and C a constant (Boundary layer thickness).

For the adsorption capacity of activated carbon, the Langmuir and Freundlich models were applied.

• Langmuir model

The solid is assumed to have a limited adsorption capacity Q_{max} linked to a limited number of adsorption sites (monomolecular layer).

The adsorption isotherms on activated carbon are described according to the Langmuir model corresponding to the equation (7).

$$q_e = \frac{q_m.K_L.c_e}{1+K_L.c_e} \quad (7)[35]$$

q_e is the quantity (mg.g^{-1}) of phenol adsorbed at equilibrium; c_e is the equilibrium concentration (mg.l^{-1}); q_m: the monolayer adsorption capacity (mg.g^{-1}); : K_L Langmuir's constant (l.mg $^{-1}$) related to the free energy of adsorption.

The linear Langmuir transform used is the relation.

$$\frac{c_e}{q_e} = \frac{1}{q_m}.c_e + \frac{1}{K_L.q_m} \quad (8)$$

• Freundlich model

This theory describes a multilayer adsorption of the adsorbate on the adsorbent surface. This isotherm is represented by the equation (9).

$$q_e = K_F.c_e^{1/n} \quad (9)[36]$$

q_e is the quantity (mg.g^{-1}) of phenol adsorbed by one gram of adsorbent; c_e is the equilibrium concentration (mg.l^{-1}); K_F et $1/n$ are the Freundlich for adsorption capacity constants (l/g) and adsorption affinity respectively.

The logarithmic form gives the linear equation (10).

$$lnq_e = lnK_F + \frac{1}{n}\,lnc_e \quad (10)$$

3. Results and Discussion

3.1. Moisture, Volatile Matter and Ash Content of Non-Activated Avocado Kernel

With a low moisture content (5.3 ± 1.2%), the avocado kernel used could have a high calorific value. The low ash content (3.5 ± 1.6%) implies that the biomass consists essentially of organic matter, i.e. the element carbon. The high volatile matter content (96.5 ± 1.6%) offers the advantages of high calorific value and a large number of functional groups [37] for the production of activated carbons. These results suggest that the avocado kernel is a good precursor for activated carbon production.

3.2. Influence of Synthesis Conditions on Activated Carbons Performance

Mass yield values decrease with increasing furnace residence time and carbonization temperature (Table 4). This is a classic thermochemical phenomenon in thermochemistry; an increase in heat or in the duration of its exposure, more of the macromolecules making up the biomass are lost. A lower yield implies an increase in the porous network due to the significant elimination of the organic part of the coal. Generally speaking, the mass yield of synthesis is inversely proportional to the loss of volatile matter.

Table 4. Mass yields and iodine value of activated carbons

Activated carbon	Synthesis yield (%)	Iodine value (mg.g^{-1})
AC_{300}-2-50	45.4	710.7
AC_{350}-2-50	40.8	930.6
AC_{400}-1-50	35.8	676.8
AC_{400}-2-20	39.4	812.2
AC_{400}-2-35	41.3	1049.1
AC_{400}-2-50	35	1167.5
AC_{400}-2-65	40.6	1302.9
AC_{400}-3-50	31.6	1150.6
AC_{400}-4-50	30.6	1184.5
AC_{450}-2-50	33.4	1235.2
AC_{500}-2-50	28.2	1286

The activated carbons prepared had iodine values ranging from 680 ± 74 mg.g^{-1} to 1300 ± 74 mg.g^{-1}. Seven (7) of the prepared activated carbons are of good quality because according to the SILEX INTERNATIONAL technical description on the quality criterion of an activated carbon, the iodine index must be higher than 950 mg.g^{-1} [25]. Comparing these values with those in the literature (Table 5), we deduce that the mass yield and the iodine value are strongly related to the biomass and activating agent.

Principal component analysis was used to study the effects of different experimental factors (carbonization temperature, furnace residence time and activating agent concentration) on the quantity and quality (synthesis mass yield and iodine value) of the activated carbons obtained. The results in Tables 6 and 7 (after varimax rotation) shows that the mass yield, the iodine value and the

carbonization temperature are strongly correlated to the factors F1 and D1; similarly, acid concentration is strongly correlated with the factors F2 and D2.

Carbonization temperature, activating agent concentration, mass yield and iodine number are strongly correlated. Increasing temperature and concentration are proportional to the iodine value. A negative effect on mass yield was observed. This is because increasing the concentration of activating agent can modify the structural characteristics and surface functional groups of the adsorbent material. On the other hand, weak correlations are observed with carbonization time. Similar correlations are found in the literature [14,23,40].

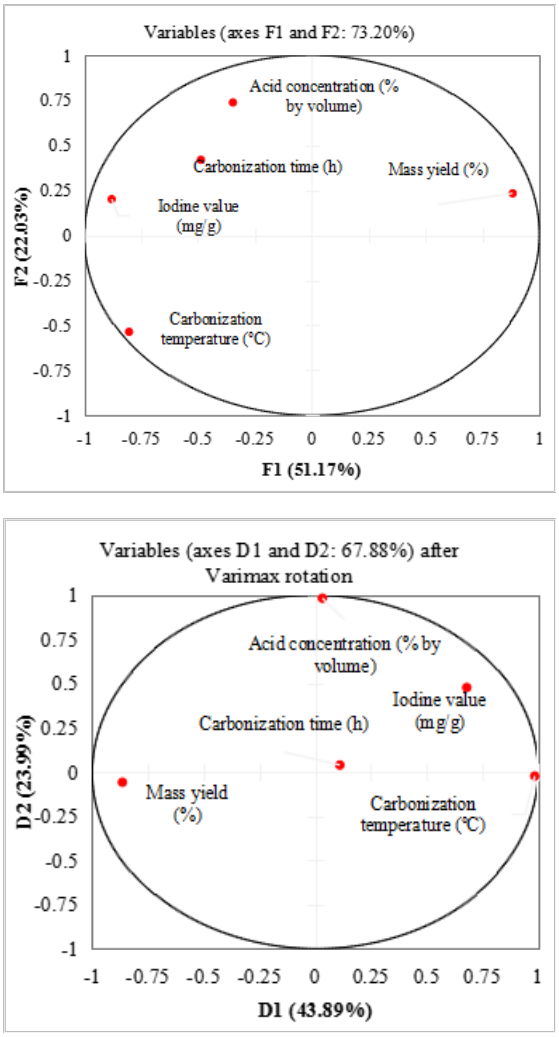

Figure 2. Correlation circles between variables and factors

Table 5. Comparisons with other activated carbons

Biomass	Activating agent	Yield (%)	Iodine value ($mg.g^{-1}$)	Reference
Coconut shell	H_3PO_4	30 - 41	432 - 870	[22]
Peanut shell	H_3PO_4	24 31 - 71	955 271 - 880	[24] [23]
Olive shell	K_2CO_3	-	1720	[38]
Pignon Pine Cones	H_3PO_4	70	466	[17]
Jujube pits	NaOH KOH	-	409 745	[39]
Avocado kernels	H_3PO_4	28 - 45	677 - 1303	This study

Table 6. Correlations between variables and factors

	F1	F2	F3	F4	F5
Carbonization temperature (°C)	-0.8036	-0.5363	-0.2257	0.0647	0.1069
Carbonization time (h)	-0.4878	0.4188	0.7632	-0.0233	0.0600
Acid concentration (% by volume)	-0.3468	0.7376	-0.5503	-0.1769	0.0382
Mass yield (%)	0.8830	0.2329	-0.0801	0.3922	0.0766
Iodine value (mg/g)	-0.8801	0.2005	-0.0804	0.4170	-0.0690

Table 7. Correlations between variables and factors after Varimax rotation

	D1	D2	D3
Carbonization temperature (°C)	0.9853	-0.0234	-0.1142
Carbonization time (h)	0.1109	0.0390	0.9910
Acid concentration (% by volume)	0.0327	0.9828	0.0162
Mass yield (%)	-0.8646	-0.0582	-0.2989
Iodine value (mg/g)	0.6804	0.4775	0.3611

3.3. Adsorption Capacity of Activated Carbons

Activated carbon with the highest specific surface area AC_{500}-2-65 was used to test phenol adsorption capacity.

3.3.1. Adsorption Kinetics

Figure 3 shows the evolution of the removal rate and the residual phenol concentration (C_e) of the solution as a function of time. Rapid adsorption is observed for the first 20 minutes, followed by slow adsorption before reaching equilibrium. The rapid adsorption observed at the start of contact could be explained by the presence of a large number of available sites on the adsorbent. But it could also be linked to the physicochemical characteristics of the material and especially to the nature of the material's porosity [41].

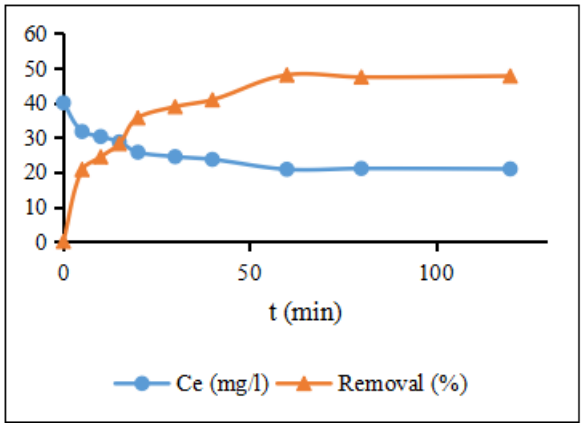

Figure 3. Influence of contact time on phenol adsorption

At the level of the slow phase that follows and leads to equilibrium, it would reflect the gradual occupation of adsorption sites on the charcoal making them less and less available. This leads to diffusion towards less accessible sites, slowing the rate of adsorption before equilibrium is reached [42] Thus, equilibrium is reached after 60 min for an adsorption capacity of 48 $mg.g^{-1}$. These results corroborate with the work of [30] on olive kernel-based carbons with an

adsorption capacity of 20 $mg.g^{-1}$, [43] on commercial activated carbon for an adsorption capacity of 70 $mg.g^{-1}$. In contrast, Kaleta (2006) obtained equilibrium at 30 min for a capacity of 61 $mg.g^{-1}$. [31] synthesized an avocado kernel-based carbon for phenol adsorption and achieded an equilibrium time of 100 min with over 98% removal.

Graphical representations of the pseudo-first order, pseudo-second order and intra-particle diffusion equations are given in Figures 4a, 4b and 4c respectively.

The various parameters of the graphical representations of the pseudo-first order, pseudo-second order and intra-particle diffusion equations are summarized in Table 8.

Analysis of Table 8 shows that the correlation coefficients (R^2) of the linear representations of the pseudo-first order and pseudo-second order equations are nearest to the value one. Furthermore, the maximum adsorption value (q_e) both obtained experimentally and theoretically using the pseudo-second order equation are closer. Therefore, the second order kinetic law is well suited to simulating the temporal evolution of the phenol concentration in solution. Similar results have been obtained by other authors such as [30,45,46] when investigating the adsorption of phenolic micro pollutants on activated carbons.

Table 8. Phenol adsorption kinetic parameters

Pseudo-first order			Pseudo-second order			Intraparticle diffusion		
qe ($mg.g^{-1}$)	k_1 (min^{-1})	R^2	qe ($mg.g^{-1}$)	k_2 ($g.mg^{-1}min^{-1}$)	R^2	K_d ($mg.g^{-1}min^{-0.5}$)	C	R^2
10.1	0.053	0.99	54.64	0.0016	0.99	5.05	9.77	0.96

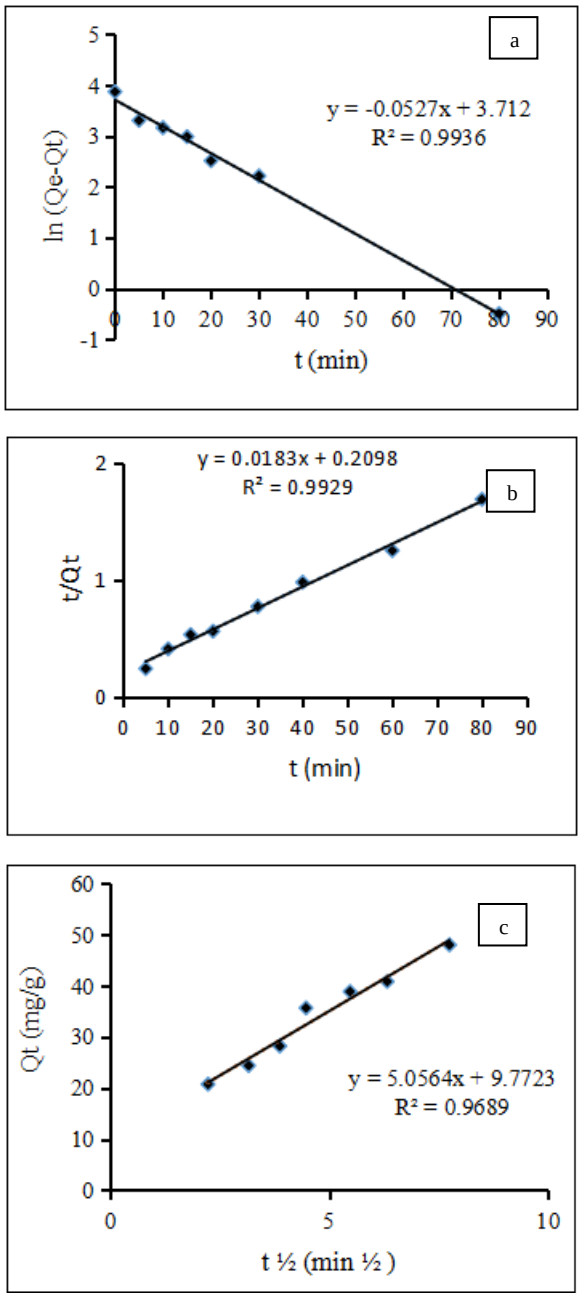

Figure 4. Kinetics of phenol adsorption

3.3.2. Study of Adsorption Isotherms

According to Giles' classification, the isotherm is type L (Langmuir class) in sub group 3 without the saturation plateau [47]. This form isotherm indicates that the adsorbent material would be essentially micro porous and that the adsorption of these compounds takes place via a monolayer chemisorption process at equivalent adsorption sites.

Figures 6a and 6b shows the isotherms applied to the Langmuir (6a) and Freundlich (6b) models for phenol adsorption.

The adsorption isotherm is perfectly described by the Langmuir model. Phenol adsorption is of the chemisorption type, with the formation of a molecular monolayer. The adsorption is located on sites of the equal energy, with no interactions between the adsorbed molecules. Similar results have been obtained by some authors on adsorbent supports from activated carbon from avocado pits [31], olive pomace [32], commercial activated carbons [43,48].

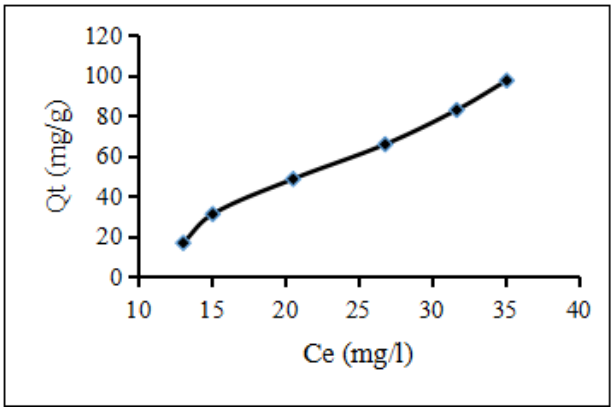

Figure 5. Phenol adsorption isotherm

Table 9. Parameters associated with the isotherms of the Langmuir and Freundlich models

	Langmuir			Freundlich		
	Qm ($mg.g^{-1}$)	K_L ($L.mg^{-1}$)	R^2	K_F ($mg.g^{-1}$)	1/n	R^2
Value	86.7	0.077	0.99	0.88	1.32	0.99

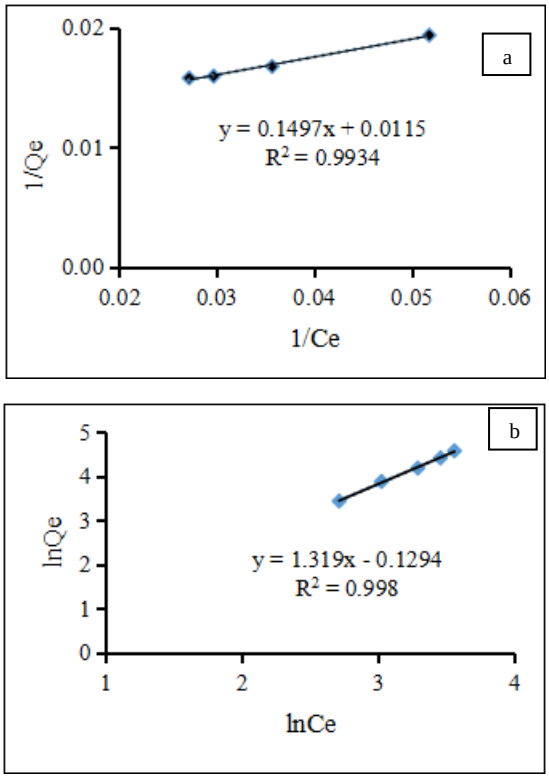

Figure 6. Modeling of phenol adsorption isotherms

4. Physical and Chemical Characteristics of Activated Carbons

Surface chemical functions and pH at zero charge point were investigated on activated carbons with the best iodine values. Table 10 shows the results obtained.

Table 10. Surface functions (meq/g) and pH at the point of zero charge of some samples

Activated carbons	Surface functions (meq/g)					
	Carboxyl.	Lacton.	Others	Total acid	Basic total	pH_{PCN}
AC_{500}-2-50	1	2	4	7	0	4.35
AC_{400}-2-65	2	2	1	5	0	2.2
AC_{400}-3-50	1	3	3	7	0	2.35

The results specify the acidic nature of the 3 activated carbons and the absence of basic groups. Similar results were obtained by [25] for activated carbons derived from the core shell of *Balanites aegyptiaca*, and by [16] for activated carbons derived from cocoa pod shells. These authors explain that the total absence of basic function is justified by the fact that the activated carbons produced were not brought in contact with oxygen below 200°C or above 700°C. Nor have they been treated with hydrogen or degassed at room temperature as this is where the basic functions are introduced.

These carbons all have zero charge pH values below neutrality; so their acidic nature is certainly linked to the activation method, which introduces a large number of acidic sites. These results show that increasing the concentration of activating agent leads to an increase in the number of carboxyl groups.

In the literature, different pH_{PCN} values are reported, which may be linked to the activation technique applied and the washing method after elaboration.

The FTIR results (Figure 7) show that the spectra of the four activated carbons are practically similar. The only relative difference observed between them is linked to the intensity of the peaks observed in comparison with the spectrum of the non-activated avocado kernel. Biomass activation has modified the chemical functions on the surface of activated carbons. The main bands are assigned as follows:

- Bands around the 3500-3000 cm^{-1} region can be attributed to elongation vibrations of the O-H hydroxyl groups, belonging to phenolic compounds and carboxylic groups.
- The peaks around 2920 cm^{-1} more intense on the non-activated core spectrum than in the charcoal spectra are due to elongation vibrations of symmetrical and asymmetrical C-H and suggests the presence of aliphatic structures in the alkanes.
- Bands around 1720-1650 cm^{-1} are usually attributed to C=O stretching vibrations of ketones, aldehydes, lactones or carboxylic groups.
- Charcoal spectra also show a strong band at 1600–1580 cm^{-1} due to vibrations of C=C bonds in aromatic rings.
- The region around 1410 cm^{-1} gives some idea of the relative abundance of the CH_2 and CH_3 groups.
- The spectrum of the non-activated nucleus shows a band in the spectral region between 1190 and 900 cm^{-1} with a maximum at 1020 cm^{-1}. This band was attributed to C–O elongation in acid, alcohol, phenol, ether, and ester groups.

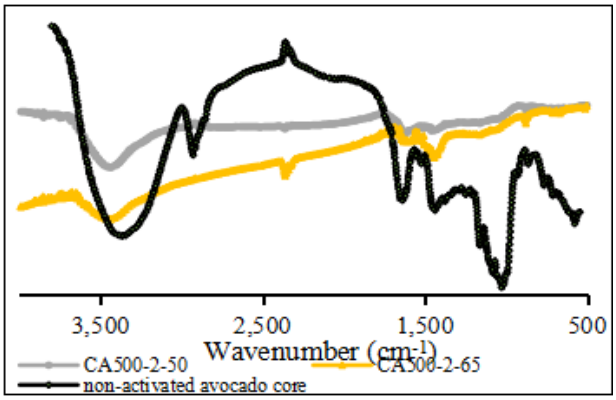

Figure 7. IR spectra for some activated carbons compared to non-activated avocado core

Interpretation of the FTIR results confirms the presence of carboxylic functional groups, lactones and phenols.

By comparing the IR spectra of activated carbons carbonized at the same temperature, we can see that the attack with the more concentrated acid results in a much more homogeneous structure compared, compared with the heterogeneity of non-activated avocado core.

Elemental analysis indicates the carbonaceous nature of the material. The results presented (Table 11) show that all these materials are essentially made up of carbon, which is consistent with activated carbons. Compared with non-activated avocado core, activated carbons have higher carbon contents. On the prepared activated carbons, it can be seen that temperature increases the carbon content at

the same time as the oxygen content decreases. These materials would contain oxygen and associated mineral elements (determined by difference). The values obtained are comparable to those in the literature.

Table 11. Comparison with the literature of the elemental compositions (in %) of some activated carbons and biomass (O* is determined by difference)

Material	C	H	N	S	O*	Reference
Avocado kernel	54.8	8.1	1.2	0	35.9	This study
Avocado kernel	46	7	0.8	-	44	[20]
AC_{500}-2-50	79.8	2.6	2.7	0	14.9	This study
AC_{400}-2-65	71.2	2.8	2.4	0	23.6	
AC_{400}-3-50	72.1	2.8	2, 6	0	22.5	
AC_{500}-2-65	75.3	2.4	1.9	0	20.4	
AC coffee grounds	68.8-75.9	3-3.3	2-2.4	< 0.2	13.5-20.7	[49]
AC coal	81.4	5	1	1.5	11.1	[50]
Avocado biochar + methylpolysiloxane composite	53.6-61.2	3-3.8	1-1.1	8-11.3	26.6-30.3	[51]

The results presented in figure 8 show that the biomass and activated carbons contain other elements such as Al, Si, P and K. Phosphorus is predominant, followed by aluminum. The other elements Fe, Mg, Cr, Na and Ti are found in trace amounts.

In addition, as the concentration of activating agent and carbonization temperature increases, so does the amount of phosphorus in activated carbons, which can be explained by the nature of the activating agent used, which is phosphoric acid.

XRD analysis of the non- activated avocado core (Figure 9) revealed crystallized forms consisting mainly of silica and quartz. On the other hand, the diffractogram of activated carbon AC_{500}-2-65 appears the single peak at 2θ = 27° characteristic of HPO_3 linked to activation with phosphoric acid. Similar observations are made on charcoals based on cotton cake and shea cake chemically activated with phosphoric acid [52].

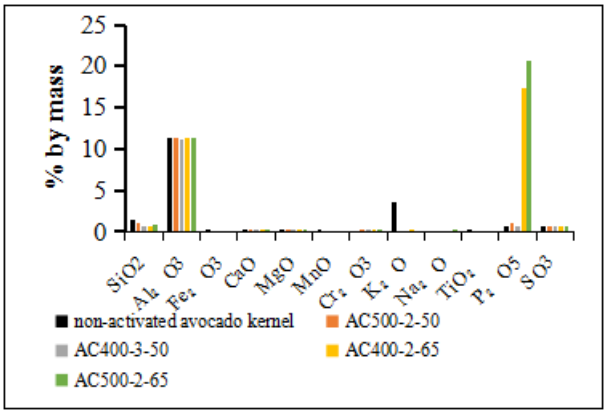

Figure 8. Elemental mineralogical composition of some activated carbons compared with non-activated avocado kernel

The SEM image is intended to illustrate porosity, especially that created by activation [53]. Scanning electron microscopy images of the activated carbon surface and the non-activated core (Figure 10) show similarities with the literature for activated carbons from avocado pits [19]. It is observed on the non-activated core, an irregular surface with scattered grains. On the other hand, SEM images of activated carbons appear relatively more homogeneous with the presence of cavities on the surface, due to heat treatment and activation.

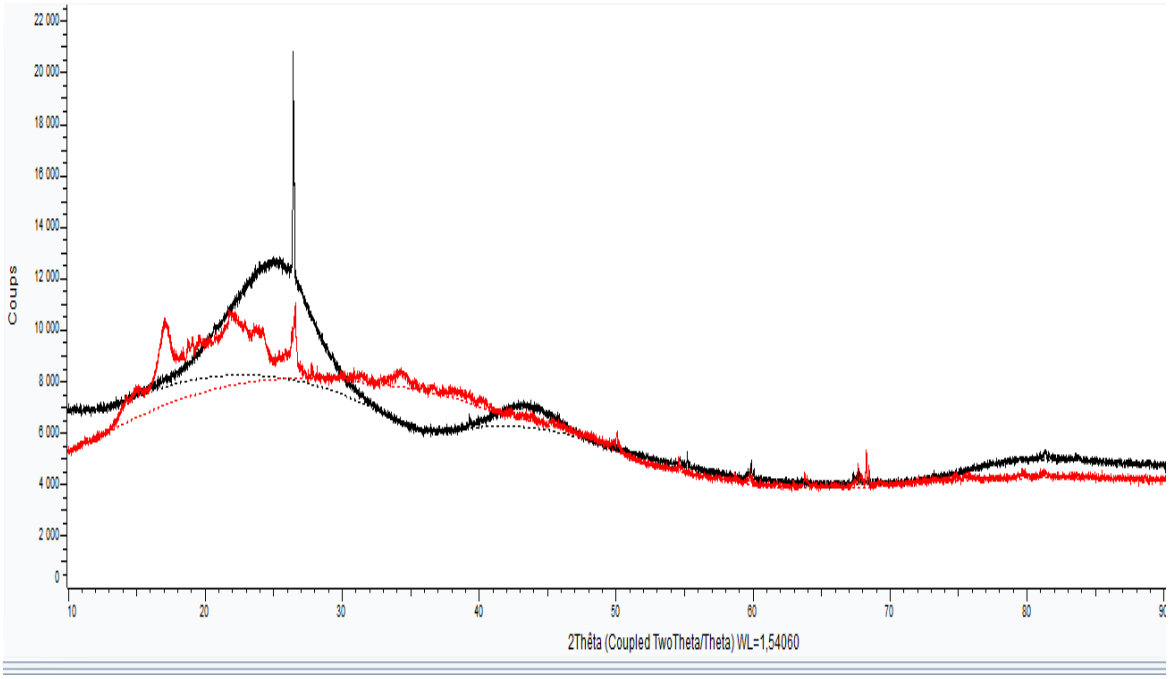

Figure 9. Diffractogram of activated carbon AC500 -2-65 (in red color) compared with non-activated avocado kernel

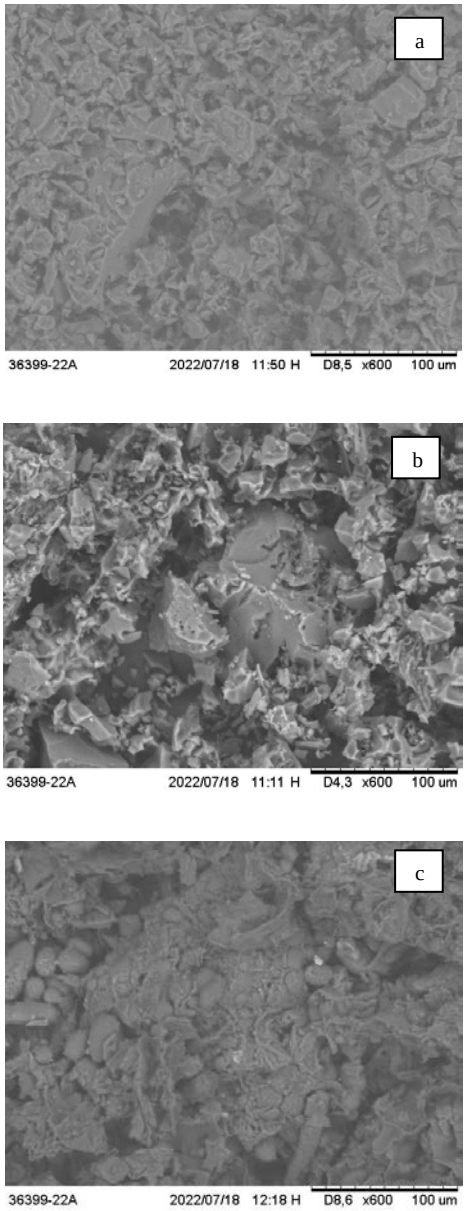

Figure 10. SEM images for activated carbons AC_{500}-2-50 (a), AC_{500}-2-65 (b) and non-activated avocado kernel (c)

The specific surface areas (S_{BET}) of some carbons was determined in order to assess their adsorption capacity. The results are shown in Table 12. These results show that AC_{500}-2-65 activated carbon has a high exchange surface. By comparing these values with those found in the literature (Table 13), we can say that this activated carbon complies with standards for the specific surface area of activated carbons, and this would justify its good adsorbent capacity. Furthermore, this activated carbon with the best specific surface area also has the highest iodine index (1506 $mg.g^{-1}$), confirming its micro porous nature.

Table 12. Specific surfaces areas of some activated carbons

Activated carbons	AC_{400}-2-65	AC_{400}-3-50	AC_{500}-2-50	AC_{500}-2-65
S_{BET} ($m^2.g^{-1}$)	94.6 ± 3	143.7 ± 5	239.3 ± 8	862.21 ± 26

Table 13. Comparison with some activated carbons from the literature

Precursor	Activating agent	Specific surface area S_{BET} ($m^2.g^{-1}$)	Reference
Avocado kernel	H_3PO_4	95-862	This study
Avocado kernel	$ZnCl_2$	1122-1584	[12]
Avocado kernel	$ZnCl_2$	1433	[18]
Avocado kernel	Physics at 900°C	700	[55]
Avocado kernel	-	206	[54]
Coconut shell	H_3PO_4	1264-1653.7	[22]
Rice husks	NaOH; H_3PO_4	19,5; 145	[55]
Date stones	HNO_3 +H_3PO_4	750-1100	[56]

From these two tables we can deduce two essential pieces of information: specific surface area increases with carbonization temperature, i.e. when material loss of is higher, and they are linked to the nature of the precursor and the synthesis conditions. Indeed, activation of avocado kernels with zinc chloride reveals higher BET surfaces areas than with hydrochloric acid. In general, activation with zinc chloride has been shown to produce activated carbons with high porosity, but due to environmental problems linked to the toxicity of residual zinc compounds, this process has been abandoned. However, it is recognized that the suitability of an activated carbon for an application depends less on specific surface area than on pore distribution. That's why this study focuses instead on developing an activated carbon with a high capacity to adsorb a broad spectrum of molecules.

In addition, AC_{600}-2-65 and AC_{700}-2-65 activated carbons were prepared and characterized using infrared spectroscopy and scanning electron microscopy to compare the effect of carbonization temperature on the surface behavior of activated carbons. The results (Figures 11 and 12) show that, under the same activation conditions, there is an evolution towards a porous network that becomes more structured as the carbonization temperature rises from 400 to 700°C.

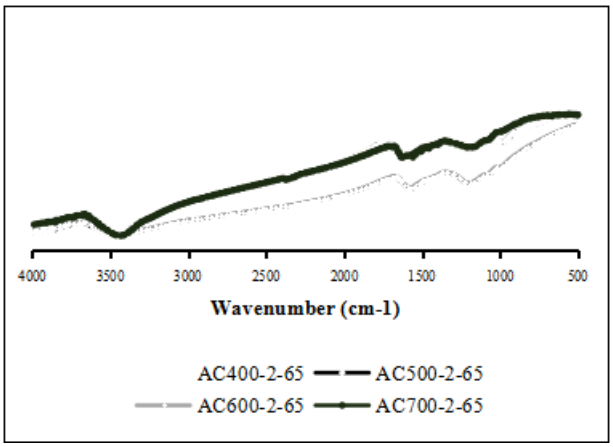

Figure 11. IR spectra of activated carbons carbonized at different temperature

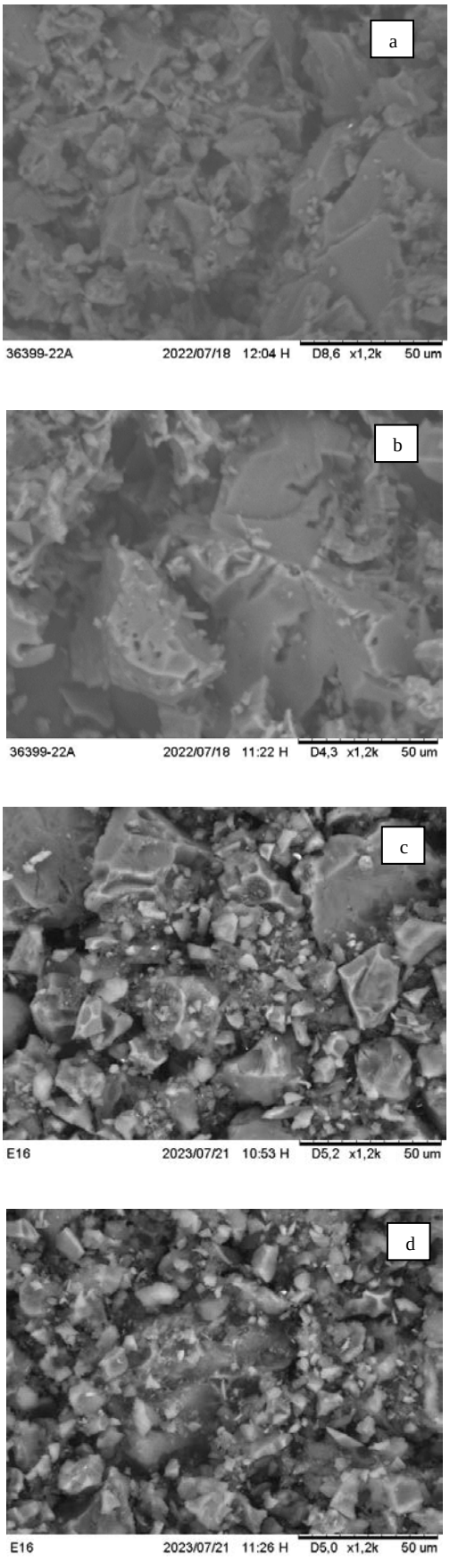

Figure 12. SEM images of activated carbons carbonized at different temperatures AC_{400}-2-65 (a), AC_{500}-2-65 (b), AC_{600}-2-65 (c) and AC_{700}-2-65 (d)

5. Conclusion

The results of this study indicate that it is possible to prepare activated carbons with interesting structural characteristics by acting on the activation parameters. The experimental study, which involved monitoring the influence of phosphoric acid concentration, carbonization temperature and carbonization time, yielded activated carbon with the maximum iodine value (1506 $mg.g^{-1}$) and BET surface area (862 $m^2.g^{-1}$), essentially micro porous under the conditions of activation with 65% phosphoric acid at a carbonization temperature of 500°C for 2 h. The study of adsorption kinetics showed that the pseudo-second-order model is the most suitable to describe phenol adsorption, implying a chemisorption-type adsorption mechanism. The high iodine values of the activated carbons we prepared indicate an interesting adsorption capacity. It is clear that some of the activated carbons produced in this study are suitable for use in the treatment.

ACKNOWLEDGEMENTS

The authors gratefully acknowledge the Cooperation and Cultural Action Department of France Embassy in Togo for funding this research works.

References

[1] Zoubeida S, Tarek B, et Anis M, «Comparison between Activated Carbon and Biochar (Theoretical Study)», University Mohammed Seddik Ben Yahia- Jijel, Algeria, Master memory, 2020.

[2] Nko'o AMC, Avom J, et Mpon R, «Evaluation of the properties of activated carbon from Moabi residue (Baillonella toxisperma Pierre) by adsorption of iodine in aqueous solution», *rseau*, vol. 29, n° 1, p. 51‑60, mars 2016.

[3] Jinyan L, « Comparative study on activated carbons », 2005.

[4] D. L. Kouadio *et al.*, «Etude expérimentale de l'adsorption du bleu 16 et du méthyle rouge sur du charbon issu de la coque de la cabosse de cacao», p. 15, 2022.

[5] N. M. Haimour et S. Emeish, «Utilization of date stones for production of activated carbon using phosphoric acid», *Waste Management*, vol. 26, n° 6, p. 651‑660, 2006.

[6] Gurten I, Ozmak M, Yagmur E, et Aktas Z, «Preparation and characterisation of activated carbon from waste tea using K2CO3», *Biomass and Bioenergy*, vol. 37, p. 73‑81, 2012.

[7] Satonaka S, Isobe T, et Kayama T, «Preparation of Activated Carbon with Phosphoric Acid from Waste Liquors, Waste Sludges and Waste from Deinking», *Hokkaido University Collection of Scholarly and Academic Papers*, vol. 41, n° 2, p. 551‑561, 2000.

[8] Abdallah M, Hijazi A, Hamieh M, Alameh M, et Rammal H, «Study of the adsorption of Methylene Blue on a biomaterial based on eucalyptus according to particle size Treatment of industrial wastewater using a natural and biodegradable adsorbent based on Eucalyptus», *Journal of Materials and Environmental Science*, vol. 7, n° 11, p. 4035‑4048, 2016.

[9] Guillaume KB, Serpokrylov NS, Smolyanichenko AS, Cheblakova EG, Gorina VA, et Yoboué DV, «Physico-chemical characteristics of the pyrolysis carbon from cashew nut shells and the activated carbons derived therefrom», *Environment, Engineering and Development*, vol. 82, p. 17‑24, 2019.

[10] Andrianaivo L, Rasoanaivo JL, et Ravoninjatovo AO, «Production of activated carbon from the endocarp of Coco Nucifera. Case of the east coast of Madagascar», *Mada-Hary, ISSN 2410-0315*, vol. 10, p. 91‑103, 2021.

[11] Guedidi H, «Preparation and modification of activated carbons for the adsorption of emerging organic pollutants: pharmaceutical molecules and ionic liquids», PhD Thesis, Grenoble, France, 2015.

[12] A. B. Leite AB *et al.*, «Activated carbons from avocado seed: optimisation and application for removal of several emerging organic compounds», *Environmental Science and Pollution Research*, vol. 25, n° 8, p. 7647‑7661, 2018.

[13] Zineb S, «Study of the effect of physicochemical parameters on the production of activated carbon from walnut shells», University Mohamed Khider of Biskra, Algeria, Master memory, 2020.

[14] Imane S, «Influence of the activation temperature on the adsorption yield of activated carbon on methylene blue», University Mohamed Khider of Biskra, Algeria, Memory of master, 2020.

[15] S. D. Maazou, H. I. Hima, M. M. M. Alma, Z. Adamou, et I. Natatou, «Elimination du chrome par du charbon actif élaboré et caractérisé à partir de la coque du noyau de Balanites aegyptiaca», *International Journal of Biological and Chemical Sciences*, vol. 11, n° 6, p. 3050‑3065, 2017.

[16] Konan KG, Meite L, Soro DB, Traore SK, et Mamadou K, «Application of an Experimental Design Methodology to Optimize the Synthesis Conditions of an Activated Carbon from Palm Kernel Shells», I*nternational Journal of Current Microbiology and Applied Sciences*, vol. 10, n° 06, p. 539‑547, 2021.

[17] Azzouz L, Belaloui D, et Bouchemal N, «Valorization of the cones of the Pine Pinus Pinea L., by the synthesis of activated carbon, characterization study», *Review Agrobiologia*, vol. 12, n° 1, p. 3000‑3008, 2022.

[18] Kudo MVF *et al.*, «Performance of avocado seed activated carbon as adsorbent for highly sensitive determination of CD using a flow injection system online coupled to TS-FF-AAS», *Journal of the Brazilian Chemical Society*, vol. 31, p. 100‑108, 2020.

[19] Zhu Y, Kolar P, Shah SB, Cheng JJ, et Lim PK, «Avocado seed-derived activated carbon for mitigation of aqueous ammonium», *Industrial Crops and Products*, vol. 92, p. 34‑41, 2016.

[20] F. Sánchez, F. Agudín, et G. San Miguel Alfaro, «Granular activated carbons from avocado seeds», 2017.

[21] Elabed A et Saoiabi A, «Thermal reactivity and kinetic degradation of argan wood: Application to the production of activated carbon by chemical activation with phosphoric acid», Thesis, Mohammed V - Agdal, Maroc, 2007.

[22] Balogoun CK, Bawa ML, Osseni S, et Aina M, «Preparation of chemically activated carbons with phosphoric acid based on coconut shell», *International Journal of Biological and Chemical Sciences*, vol. 9, n° 1, p. 563‑580, 2015.

[23] M. Gueye, J. Blin, et C. Brunschwig, «Etude de la synthèse des charbons actifs à partir de biomasses locales par activation chimique avec H3PO4», *des journées scientifiques du 2IE*, 2011.

[24] Kouadio DL, Djassou AC, Koffi ALC, et Sory K, «Development of materials for environmental pollution control from cocoa pod shells», *International Journal of Engineering and Applied Sciences*, vol. 6, p. 40‑45, 2019.

[25] Maazou SDB, Hima HI, Alma MMM, Adamou Z, et Natatou I, «Elimination of the chromium by the elaborate activated coal and characterized from the c-ockle of the core of Balanites aegyptiaca.», *International Journal of Biological and Chemical Sciences*, vol. 11, n° 6, p. 3050‑3065, 2017.

[26] Lopez-Ramon MV, Stoeckli F, Moreno-Castilla C, et Carrasco-Marin F, «On the characterization of acidic and basic surface sites on carbons by various techniques», *Carbon*, vol. 37, n° 8, p. 1215‑1221, 1999.

[27] Boehm HP et Scholz W, «Investigations on graphite oxide, Comparison of the preparation methods for graphite oxide», *Justus Liebig's Annals of Chemistry*, vol. 691, n° 1, p. 1‑8, 1966.

[28] R.-L. Tseng et S.-K. Tseng, «Characterization and use of high surface area activated carbons prepared from cane pith for liquid-phase adsorption», *J Hazard Mater*, vol. 136, n° 3, p. 671‑680, août 2006.

[29] Bellam B, «Study of the removal of 2, 4, 5 Trichlorophenol on commercial activated carbon synthesized from coffee grounds», PhD Thesis, Sétif 1 Ferhat Abbas, Algeria, 2018.

[30] Bohli T, Fiol Santaló N, Villaescusa GI, et Ouederni A, «Adsorption on activated carbon from olive stones: kinetics and equilibrium of phenol removal from aqueous solution», *Journal of Chemical Engineering and Process Technology*, vol. 4, n° 6, p. 5, 2013.

[31] Kassahun D, Khalid S, et Shimeles AK, «Kinetic and thermodynamic study of phenol removal from water using activated carbon synthesizes from Avocado kernel seed», *International Letters of Natural Sciences*, vol. 54, p. 42‑57, 2016.

[32] N. Naib, «Study of the phenol adsorption process on activated carbon based on olive pomace modeling by experimental plans», PhD Thesis, M'hamed Bougara, Algeria, 2007.

[33] Mahugo SC, Sosa FZ, Esther TDM, et Juan SRJ, «Methodologies for the Extraction of Phenolic Compounds from Environmental Samples: New Approaches», *Molecules*, vol. 14, n° 1, Art. n° 1, janv. 2009.

[34] S. K. Lagergren, «About the theory of so-called adsorption of soluble substances», *Sven. Vetenskapsakad. Handingarl*, vol. 24, p. 1‑39, 1898.

[35] I. Langmuir, «The adsorption of gases on plane surfaces of glass, mica and platinum.», *Journal of the American Chemical society*, vol. 40, n° 9, p. 1361‑1403, 1918.

[36] H. Freundlich, «Über die adsorption in lösungen», *Zeitschrift für physikalische Chemie*, vol. 57, n° 1, p. 385‑470, 1907.

[37] Mbaye G, «Synthesis and studies of activated carbons for the treatment of wastewater from a tannery», 2iE Burkina Faso, Master in energy and industrial processes, 2009.

[38] Petrov N, Budinova T, Razvigorova M, Parra J, et Galiatsatou P, «Conversion of olive wastes to volatiles and carbon adsorbents», Biomass and Bioenergy, 32: 1303-1310.

[39] Zohra B, «Activation of jujube kernels to obtain activated carbon», Thesis, University Abdelhamid Ibn Badis Mostaganeme, Algeria, 2018.

[40] Tchakala I, Bawa LM, Djaneye-Boundjou G, Doni KS, et Nambo P, «Optimization of the process for preparing Activated Carbons by chemical means (H3PO4) from Shea cake and cotton cake», *International Journal of Biological and Chemical Sciences*, vol. 6, n° 1, p. 461‑478, 2012.

[41] K. N. Aboua, D. B. Soro, M. Diarra, K. Bibi, K. R. N'Guettia, et K. S. Traoré, «Étude de l'adsorption du colorant orange de méthyle sur charbons actifs en milieu aqueux: influence de la concentration de l'agent chimique d'activation», *Afrique science*, vol. 14, n° 6, p. 322‑331, 2018.

[42] Joseph O, «Study of the potential for using Haitian agricultural residues for the biosorption treatment of polluted effluents», PhD Thesis, INSA Lyon, France, 2009.

[43] Kessoum M, Caqueret V, Chedeville O, Cagnon B, Bostyn S, et Porte C, «Study of the kinetics and thermodynamics of adsorption of phenolic compounds in monosolutes and in mixtures on activated carbon», 2014.

[44] Kaleta J, «Removal of phenol from aqueous solution by adsorption», *Canadian Journal of Civil Engineering*, vol. 33, n° 5, p. 546‑551, 2006.

[45] Aziz A, Yusop MFM, et Ahmad MA, «Removal of Bisphenol S from Aqueous Solution using Activated Carbon Derived from Rambutan Peel via Microwave Irradiation Technique», *Sains Malaysiana*, vol. 51, n° 12, p. 3967‑3980, 2022.

[46] Mishra L, Paul KK, et Jena S, «Adsorption Isotherm, Kinetics and Optimization Study by Box Behnken Design on Removal of Phenol from Coke Wastewater Using Banana Peel (Musa sp.) Biosorbent», *Theoretical Foundations of Chemical Engineering*, vol. 56, n° 6, p. 1189‑1203, 2022.

[47] C. H. Giles, D. Smith, et A. Huitson, «A general treatment and classification of the solute adsorption isotherm. I. Theoretical», *Journal of Colloid and Interface Science*, vol. 47, n° 3, p. 755‑765, juin 1974.

[48] Özkaya B, «Adsorption and desorption of phenol on activated carbon and a comparison of isotherm models», *Journal of Hazardous Materials*, vol. 129, n° 1, p. 158‑163, 2006.

[49] A. Reffas, E. M. Bencheikh, et L. Duclaux, «Étude de l'adsorption de colorants organiques (rouge nylosan et bleu de méthylène) sur des charbons actifs préparés à partir du marc de café», 2010.

[50] Zaabal M, «Study of the adsorption properties of porous materials based on linocellulose and carbon derivatives», Memory of master, University of Houari Boumediene, Algeria, 2012.

[51] Teixeira RA, «Composite of methyl polysiloxane and avocado biochar as adsorbent for removal of ciprofloxacin from waters», *Environmental Science and Pollution Research*, p. 18, 2022.

[52] I. Tchakala, «Contribution à l'étude de la préparation des charbons actifs à partir des résidus carbonés des industries de transformation agroalimentaires (cas des tourteaux de karité et des tourteaux de coton) : caractérisation et applications en traitement des eaux», Lomé, 2013.

[53] M. Trachi, N. Bourfis, S. Benamara, et H. Gougam, «Préparation et caractérisation d'un charbon actif à partir de la coquille d'amande (Prunus amygdalus) amère», *Biotechnol. Agron. Soc. Environ.*, p. 11, 2014.

[54] Rodrigues LA, da Silva MLC, Alvarez-Mendes M, dos Reis CA, et Thim GP, «Phenol removal from aqueous solution by activated carbon produced from avocado kernel seeds», *Chemical Engineering Journal*, vol. 174, n° 1, p. 49‑57, 2011.

[55] Sanou Y, Ségbéaya KN, Paré S, Baba G, et Bonzi-Coulibaly LY, «Experimental study of the elimination of calcium from wastewater by mesoporous activated carbons», *Journal of the West African Society of Chemistry*, vol. 47, p. 52‑60, 2019.

[56] Hazourli S, Ziati M, Hazourli A, et Cherifi M, «Valorization of a natural lignocellulosic residue into activated carbon - example of date stones», *Renewable Energy Review, ICRESD*, vol. 7, p. 187‑192, 2007.